nation step. A great amount of heat was given off, causing the THF to reflux during the time the solid isopropyltrihydroborate was dissolving, so slow addition of THF was necessary.

Cyanation went more quickly and at lower temperatures than for isobutyltrihydroborate, probably due to a stronger inductive effect of the secondary carbon of the isopropyl group. The method of at first using a deficiency reaction followed by adding the remainder of required $Hg(CN)_2$ to complete the reaction worked well. Advantage was taken of the apparent order of reactivity of hydroborates with $Hg(CN)_2$: $RBH_3^- > BH_4^- > RBH_2CN^- > BH_3CN^-$, allowing for complete conversion to the desired isopropylcyanodihydroborate, without either the dicyanation product or uncyanated i-$PrBH_3^-$ being present. A ^{11}B NMR spectrum taken of the amine–isopropylcyanoborane products (**6a** and **7a**) revealed that neither over- nor undercyanation had occurred on the isopropyltrihydroborate center and that the tetrahydroborate byproduct had been approximately half-cyanated to give BH_3CN^-.

The pyridine adduct **6a** was a liquid that solidified at approximately 10 °C. Since a small amount of isopropylboronic acid was present in **6a** (as indicated in the ^{11}B NMR spectrum), no elemental analysis was obtained. The carbamoylborane product formed from **6a** proved to have a good elemental analysis, showing that pyridine–isopropylcyanoborane had indeed been synthesized as an intermediate.

The other adduct was the quinuclidine-containing product **7a**. This proved to be a crystalline solid, and it was the first quinuclidine adduct that was directly isolated without the use of column chromatography. After recrystallization to a sandlike colorless crystalline solid that melted at 132–134 °C, a good elemental analysis indicated successful purification of this derivative. Work on the purification of **7c** continues.

Biological Activity. Samples of several of these new compounds have been submitted to Professor Iris Hall (School of Pharmacy, University of North Carolina, Chapel Hill, NC) for biological testing. Preliminary results indicate that these amine–alkylborane derivatives have similar hypolipidemic activity in general to that reported previously for the glycine boron analogues.[2c,26] Some of the new compounds were found to have antiinflammatory activity that was more effective than indomethacin. Of most significance was the antineoplastic activity of selected compounds in vitro with respect to certain murine and human cell lines. In certain cases the cytotoxicity (ED_{50} μg/mL) values were better than those of 5-fluorouracil. A full report of this pharmacological activity will be published in the near future.

Acknowledgment. This work was supported by the U. S. Army Research Office and The Public Health Service.

Registry No. **1a**, 124287-27-0; **1b**, 131236-93-6; **1c**, 131250-02-7; **2a**, 124287-29-2; **2b**, 131250-01-6; **2c**, 131237-00-8; **3a**, 124287-33-8; **3b**, 125844-06-6; **3c**, 125844-02-2; **4a**, 124287-30-5; **4b**, 131236-95-8; **4c**, 131237-01-9; **5a**, 124287-31-6; **5b**, 131236-97-0; **5c**, 131237-02-0; **6a**, 131236-90-3; **6b**, 131236-99-2; **6c**, 131237-03-1; **7a**, 131236-91-4; *i*-PrLi, 1888-75-1; $Me_2S{\cdot}BH_3$, 13292-87-0; Et_3OBF_4, 368-39-8; lithium isopropyltrihydroborate, 84280-38-6; lithium isopropylcyanodihydroborate, 131236-89-0; pyridine hydrochloride, 628-13-7; quinuclidine, 100-76-5.

(26) Hall, I. H.; Spielvogel, B. F.; Sood, A.; Ahmed, F.; Jafri, S. *J. Pharm. Sci.* **1987**, *76*, 359.

Contribution from the Department of Chemistry, University of Massachusetts, Amherst, Massachusetts 01003

Conformational Effects of Ring Fusion and Heteroatom Substitution in Six-Membered Rings of Spirocyclic Oxyphosphoranes[1,2a]

Robert R. Holmes,* K. C. Kumara Swamy, Joan M. Holmes, and Roberta O. Day

Received July 31, 1990

Spirocyclic oxyphosphoranes containing six-membered rings **1–5** were synthesized by oxidative addition of cyclic phosphites with phenanthrenequinone. Substituent variations in **1–5** allowed the examination of the conformational stability of the six-membered ring system. This ring in **4** was trans annelated with cyclopentane, established by X-ray analysis. The latter feature has relevance to c-AMP. A cis-fused phosphorinane derivative containing a furanose ligand **7** was also prepared. X-ray structures revealed trigonal-bipyramidal frameworks with the phosphorinane ring occupying apical–equatorial positions. The saturated six-membered ring was uniformly in a boat conformation. Despite considerable electronegativity and ring substituent effects, no diequatorial ring placement was evident. Variable-temperature ^1H NMR data indicated retention of solid-state structures in solution. Rapid pseudorotation is indicated for the various phosphoranes with the thio derivative **2** appearing more fluxional. Analogies with models for cyclic AMP action are discussed. Phosphorane **1** crystallizes in the orthorhombic space group $P2_12_12_1$ with a = 7.769 (2) Å, b = 10.191 (2) Å, c = 29.594 (5) Å, and Z = 4. The thiophosphorane **2** crystallizes in the orthorhombic space group $P2_12_12_1$ with a = 7.696 (1) Å, b = 10.441 (2) Å, c = 30.130 (6) Å, and Z = 4. The diaminophosphorane **3** crystallizes in the triclinic space group $P\bar{1}$ with a = 10.078 (3) Å, b = 10.133 (3) Å, c = 12.253 (3) Å, α = 101.60 (2)°, β = 92.81 (2)°, γ = 105.00 (2)°, and Z = 2. The fused-ring phosphorane **4** crystallizes in the monoclinic space group $P2_1/c$ with a = 15.147 (3) Å, b = 9.092 (2) Å, c = 18.089 (4) Å, β = 108.92°, and Z = 4. The final conventional unweighted residuals are 0.037 (**1**), 0.036 (**2**), 0.040 (**3**), and 0.040 (**4**).

Introduction

In recent studies on monocyclic and spirocyclic oxyphosphorane compounds,[2-5] we have found that the structures assumed trigonal-bipyramidal forms with the rings, which varied from five- to eight-membered, spanning apical–equatorial positions. For saturated six-membered rings, the preferred conformation is that of a boat with the axial atom at the prow of the boat and the opposing carbon atom at the stern. The latter observation agrees with model considerations presented earlier by Trippett,[6] from which he concluded that the boat conformation is the only one that allows the lone pair on the equatorial atom to be in the favored equatorial plane.

(1) (a) Pentacoordinated Molecules. 84. (b) Part 83: Deiters, J. A.; Holmes, R. R. *J. Am. Chem. Soc.* **1990**, *112*, 7197.
(2) (a) Kumara Swamy, K. C.; Burton, S. D.; Holmes, J. M.; Day, R. O.; Holmes, R. R. Presented in part at the XI International Conference on Phosphorus Chemistry, Tallinn, Estonia (SSR/USSR), July 1989; Abstract 2-22. (b) Burton, S. D.; Kumara Swamy, K. C.; Holmes, J. M.; Day, R. O.; Holmes, R. R. *J. Am. Chem. Soc.* **1990**, *112*, 6104.
(3) Kumara Swamy, K. C.; Holmes, J. M.; Day, R. O.; Holmes, R. R. *J. Am. Chem. Soc.* **1990**, *112*, 6092.
(4) Kumara Swamy, K. C.; Day, R. O.; Holmes, J. M.; Holmes, R. R. *J. Am. Chem. Soc.* **1990**, *112*, 6095.
(5) Kumara Swamy, K. C.; Burton, S. D.; Holmes, J. M.; Day, R. O.; Holmes, R. R. *Phosphorus, Sulfur, Silicon* **1990**, *53*, 437.
(6) Trippett, S. *Pure Appl. Chem.* **1974**, *40*, 595.

0020-1669/91/1330-1052$02.50/0 © 1991 American Chemical Society

Estimates of strain energy for rings are available from variable-temperature NMR data[6] on cyclic phosphoranes exhibiting ligand exchange via postulated high-energy intermediates that place the ring in a diequatorial location, e.g.,

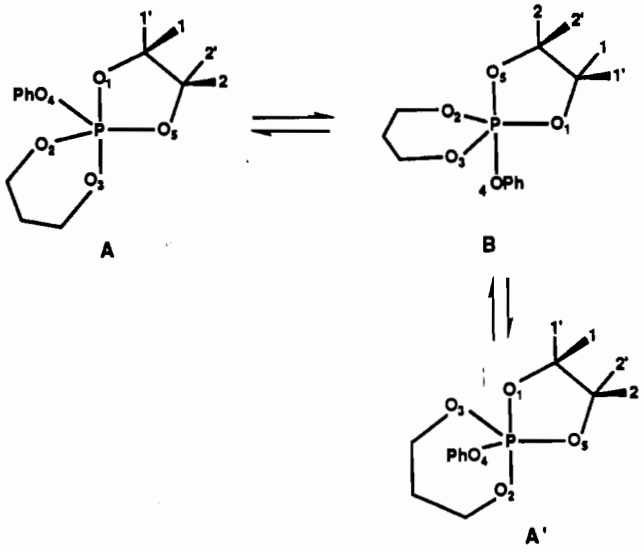

From a partitioning of energy terms Trippett[6] was led to an expression of the activation energy for the exchange process, A $\rightleftharpoons$ B $\rightleftharpoons$ A′ (eq 1), where ΔA(Y–L) is an apicophilicity term

$$\Delta G^{\ddagger} = E_B - E_A = S + R^X + R^Y + \Delta A(\text{Y–L}) \qquad (1)$$

associated with replacing the ring apical oxygen (Y = O_3) by the acyclic phenoxy group (L = O_4Ph), R^X and R^Y measure the energy required to rotate the lone pair on X and Y from the equatorial plane to the apical plane (X = O_2), and S is the ring strain encountered on going from A to B. On comparison of activation energies for the exchange process A $\rightleftharpoons$ B $\rightleftharpoons$ A′ for the related derivatives C and D,[6] ring strain differences between the two ring

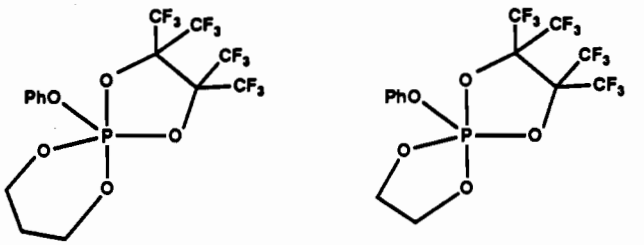

locations in A and B appear to be much less for the six-membered-ring derivative C compared to that for the five-membered-ring derivative D. Although reliable values of R^O are not available[6,7] (X = Y), these terms are approximately the same for both phosphoranes C and D. Further, the apicophilicity difference, ΔA(PhO–alkO), is small (Trippett[6] estimates 1 kcal/mol). Hence, the difference in activation energies for D – C suggests that the six-membered ring in C is stabilized in the diequatorial conformation by about 11 kcal/mol compared to that for the five-membered-ring system in D. On the basis of rough estimates for R^O, Trippett[6] suggests that the strain energy for the six-membered ring in the diequatorial position of a TBP may be nil.

It is apparent that six-membered rings offer the greater likelihood of being stabilized in diequatorial sites of trigonal bipyramids for oxyphosphoranes compared to five-membered rings. To date, however, no structure of this kind has been definitively established by X-ray diffraction, although several indications of such structures have been reported on the basis of calculations and NMR data.[8-13]

(7) Bone, S. A.; Trippett, S.; Whittle, P. J. *J. Chem. Soc., Perkin Trans 1* **1977**, 80.

Especially pertinent are model intermediates proposed for cyclic AMP action. In the activation of protein kinases by c-AMP, CNDO/2 calculations[8,9] support diequatorial placement of the six-membered cyclophosphate ring proposed to result from enzyme attack to yield a covalent complex.

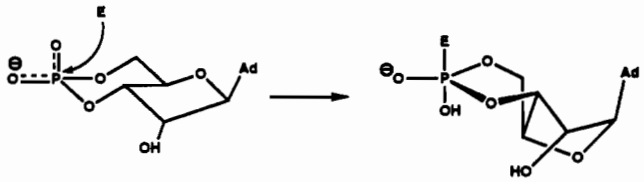

In a further theoretical investigation, van Ool and Buck[9] conclude that hydrolysis of c-AMP with phosphorodiesterase involves a TBP intermediate with an apical–equatorial ring orientation and the 3′-oxygen atom residing at an apical site. However, it is not known what factors are specific in influencing one structure over another.

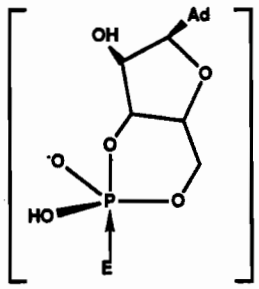

In view of the rather meager experimental data on which to base such decisions and more generally to discuss possible intermediates in reactions involving cyclic oxyphosphoranes with six-membered rings, we have examined a number of new members of this class designed with a common ligand component that will allow the isolation of specific features for evaluation. As a consequence, an assessment of important factors governing structural preferences should result.

The examples chosen in this study are the bicyclic derivatives **1–4** containing the dioxyphenanthrene ring. The presence of a

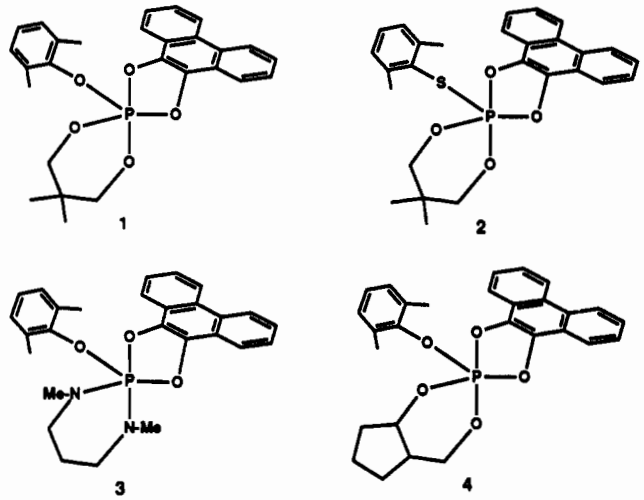

phosphorus-bonded sulfur atom in place of an oxygen atom in the

(8) van Ool, P. J. J. M.; Buck, H. M. *Recl. Trav. Chim. Pays-Bas* **1981**, *100*, 79.
(9) van Ool, P. J. J. M.; Buck, H. M. *Eur. J. Biochem.* **1982**, *121*, 329.
(10) (a) Ramirez, F.; Ugi, I. *Bull. Soc. Chim. Fr.* **1974**, 453. (b) Gillespie, P.; Ramirez, F.; Ugi, I.; Marquarding, D. *Angew. Chem., Int. Ed. Engl.* **1973**, *12*, 91.
(11) (a) Gorenstein, D. G.; Rowell, R.; Findley, J. *J. Am. Chem. Soc.* **1980**, *102*, 5077. (b) Rowell, R.; Gorenstein, D. G. *J. Am. Chem. Soc.* **1981**, *103*, 5894.
(12) Gorenstein, D. G. *Chem. Phys.* **1987**, *87*, 1047.
(13) See also ref 5, which is a recent review on cyclic oxyphosphoranes.

acyclic component is compared in derivatives **1** and **2**. The inclusion of a diazaphosphorinane ring in **3** in place of the related dioxaphosphorinane ring in **1** allows the influence of nitrogen heteroatoms to be compared with oxygen ring atoms. The latter comparison is made more significant by an earlier study that reported the structure of the corresponding sulfur derivative E.[3] For these oxyphosphoranes **1–4**, single-crystal X-ray analyses and variable-temperature NMR studies are reported.

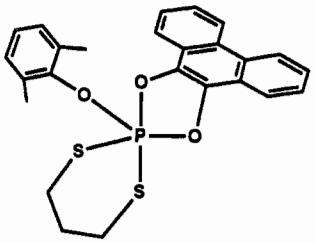

E

In addition, NMR measurements on the tetraoxyphosphorane **5**, the trans-annelated deoxythymidine cyclic pentaoxyphosphorane **6**, and the cis-fused xylofuranosylphosphorane **7** were carried out

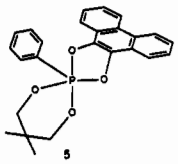

5

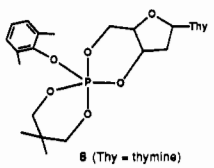

6 (Thy = thymine)

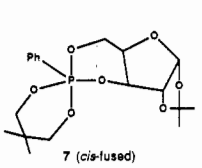

7 (*cis*-fused)

although the lack of suitable crystals prevented structural determination by X-ray diffraction. The trans-annelated derivative **6** contains the five-membered and six-membered rings of deoxythymidine fused in the same fashion as found in c-AMP, i.e., trans, whereas for **7** these rings are fused in a cis fashion. All of the phosphoranes, **1–7**, represent new compounds.

Experimental Section

Chemicals were obtained from Aldrich, Fisher Scientific, or Fluka and used without further purification. Solvents were of HPLC grade (Fisher Scientific). Further purification was done according to standard procedures.[14a,b]

^{1}H NMR spectra were recorded on a Varian Associates XL 300 or a Varian Associates XL 200 FT-NMR spectrometer. ^{31}P NMR spectra were recorded on the Varian Associates XL 300 FT-NMR spectrometer. Chemical shifts for ^{31}P NMR spectra were obtained by setting triphenyl phosphate ($CDCl_3$) at −18.0 ppm[14c] and are referenced to 85% H_3PO_4 with negative shifts upfield. Spectra were obtained at 23 °C unless otherwise stated.

Syntheses. (9,10-Phenanthrenediyldioxy)(2,6-dimethylphenoxy)((2,2-dimethyl-1,3-propanediyl)dioxy)phosphorane, ($C_{14}H_8O_2$)(Xyl–O)P($Me_2C_3H_4O_2$) (1). A mixture of 2-(2,6-dimethylphenoxy)-5,5-dimethyl-1,3,2-dioxaphosphorinane (2.86 g, 11.3 mmol), prepared as described earlier,[4] and phenanthrenequinone (2.35 g, 11.3 mmol) was kept at 100 °C for 8 min under an atmosphere of nitrogen. After cooling, the mixture was dissolved in diethyl ether (150 mL) and filtered under nitrogen. The solvent volume was reduced to 80 mL and the mixture heated to dissolve the precipitate. Preserving the solution at 20 °C unperturbed for 24 h afforded pale red crystals of **1** (3.30 g, 63%), mp 150–151 °C. ^{1}H NMR ($C_6D_5CD_3$, ppm): 0.59 (s, 3 H, $CH_2C(CH_3)_2$), 0.76 (s, 3 H, $CH_2C(CH_3)_2$), 2.31 (s, 6 H, $OC_6H_3CCH_3)_2$), 3.79 (dd, $^3J(P–H_B)$ = 19.0 Hz, $^2J(H_A–H_B)$ = 10.4 Hz, 2 H, OCH_2(B)), 3.93 (dd, $^3J(P–H_B)$ = 16.9 Hz, $^2J(H_A–H_B)$ = 10.9 Hz, 2 H, OCH_2(A)), 6.70–6.80 (m, 3 H, H(Ar)), 7.20–7.40 (m, 4 H, H(Ar)), 8.00 (d, 2 H, H(Ar)), 8.30 (d, 2 H, H(Ar)). Changing the solvent to $CDCl_3$ produced significant proton chemical shifts compared to the use of $C_6D_5CD_3$. ^{1}H NMR ($CDCl_3$, ppm): 1.12 (s, 3 H, $CH_2C(CH_3)_2$), 1.15 (s, 3 H, $CH_2C(CH_3)_2$), 2.27 (s, 6 H, $OC_6H_3(CH_3)_2$), 4.13 (dd, $^3J(P–H_B)$ = 19.1 Hz, $^2J(H_A–H_B)$ = 10.9 Hz, 2 H, OCH_2(B)), 4.27 (dd, $^3J(P–H_A)$ = 17.0 Hz, $^2J(H_A–H_B)$ = 10.9 Hz, 2 H, OCH_2(A)), 6.75–6.95 (m, 3 H, H(Ar)), 7.45–7.60 (m, 4 H, H(Ar)), 7.82 (d, 2 H, H(Ar)), 8.65 (d, 2 H, H(Ar)). ^{31}P NMR (C_6D_6): −48.96 ppm. Anal. Calcd for $C_{27}H_{27}O_5P$: C, 70.13; H, 5.84. Found: C, 70.06; H, 5.70.

Variable-temperature ^{1}H NMR spectra were recorded in the range −78 to +90 °C at 300 MHz and down to −95 °C at 200 MHz.

2-(2,6-Dimethylthiophenoxy)-5,5-dimethyl-1,3,2-dioxaphosphorinane, ($Me_2C_3H_4O_2$)P(S–Xyl) (8). To a solution of 2,6-dimethylthiophenol (4.61 g, 33.4 mmol) and 2-chloro-5,5-dimethyl-1,3,2-dioxaphosphorinane[15] (5.63 g, 33.4 mmol) in diethyl ether (150 mL) maintained at 0 °C was added slowly (10 min) triethyl amine (7.00 mL, 5.08 g, 50.2 mmol) under an atmosphere of nitrogen. The mixture was brought to 20 °C and stirred at this temperature for 14 h. It was then filtered under a nitrogen atmosphere and the solvent evaporated at 20 °C by passing a strong current of nitrogen over it to yield **8** as a solid, mp 65–67 °C (7.0 g, 78%). ^{1}H NMR ($CDCl_3$, ppm): 0.83 (s, 3 H, $CH_2C(CH_3)_2$), 1.27 (s, 3 H, $CH_2C(CH_3)_2$), 2.48 (s, 6 H, $OC_6H_3(CH_3)_2$), 3.66 (t, 2 H, OCH_2(A)), 4.30 (dd, 2 H, OCH_2(B)), 7.12 (m, 3 H, H(Ar)). ^{31}P NMR ($CDCl_3$, ppm): 169.44. Anal. Calcd for $C_{13}H_{19}O_2PS$: C, 57.78; H, 7.03. Found: C, 57.71; H, 7.03.

(9,10-Phenanthrenediyldioxy)(2,6-dimethylthiophenoxy)((2,2-dimethyl-1,3-propanediyl)dioxy)phosphorane, ($C_{14}H_8O_2$)(Xyl–S)P($Me_2C_3H_4O_2$) (2). A mixture of **8** (1.58 g, 5.85 mmol) and phenanthrenequinone (1.22 g, 5.85 mmol) was heated at 145 °C for 10 min and cooled, and the resulting solid was dissolved in dichloromethane (40 mL). Slow evaporation of the solvent afforded **2** as a crystalline solid, mp 168–171 °C (1.30 g, 46%). ^{1}H 200-MHz NMR ($C_6D_5CD_3$, ppm): 0.62 (s, 3 H, $CH_2C(CH_3)_2$), 0.71 (s, 3 H, $CH_2C(CH_3)_2$), 2.48 (d, J = 4 Hz, 6 H, $SC_6H_3(CH_3)_2$), 3.76 (dd, $^3J(P–H_B)$ = 17.4 Hz, $^2J(H_A–H_B)$ = 11.0 Hz, 2 H, OCH_2(B)), 3.87 (dd, $^3J((P–H_A)$ = 18.3 Hz, $^2J(H_A–H_B)$ = 10.9 Hz, 2 H, OCH_2(A)), 6.70–8.40 (m, 11 H, H(Ar)). ^{31}P NMR ($CDCl_3$, ppm): −20.30. Anal. Calcd for $C_{27}H_{27}O_4PS$: C, 67.75; H, 5.65. Found: C, 67.92; H, 5.57.

Variable-temperature ^{1}H NMR spectra were recorded at 200 MHz from −95 to +100 °C. At ≤−60 °C broadening of all signals was observed. At ca. −95 °C, two broad siangls for OCH_2 protons (3.70, 4.10 ppm) and $OC_6H_3(Me)_2$ protons (3.00, 1.90 ppm) were observed. At +70 °C, for OCH_2 protons a clean doublet was observed (3.83 ppm; $^3J(P–H)$ = 17.8 Hz). However, the $CH_2C(CH_3)_2$ protons were still observed as separate signals ($\Delta\delta$ = 0.06 ppm).

2-(2,6-Dimethylphenoxy)-1,3-dimethyl-1,3,2-diazaphosphorinane, ($C_3H_6Me_2N_2$)P(O–Xyl) (9). To a mixture of 2-chloro-1,3-dimethyl-1,3,2-diazaphosphorinane, ($C_3H_6Me_2N_2$)PCl (5.58 g, 33.5 mmol) prepared according to Hutchins et al.,[16] and 2,6-dimethylphenol (5.58 g, 45.7 mmol) in diethyl ether (150 mL) at 20 °C was added triethylamine (5.80 g, 57.5 mmol) with continuous stirring under a nitrogen atmosphere. The mixture was stirred overnight and filtered under nitrogen. The volatiles were removed from the filtrate and the residue distilled in vacuo to obtain **9**, bp 140 °C/0.4–0.5 mm (2.5 g, 30%). ^{1}H NMR ($CDCl_3$, ppm): 1.90–2.12 (m, 2 H, CCH_2), 2.35 (s, 6 H, CCH_3), 2.68, 2.76 (singlet each or a doublet with $^3J(P–H)$ = 15.6 Hz; 6 H, NCH_3), 2.60–2.90 (m, 2 H, NCH_2), 3.20–3.50 (m, 2 H, NCH_2), 6.60–7.10 (m, 3 H, H(Ar)). An additional peak at 2.25 ppm ($(OC_6H_3(CH_3)_2$, ca. 5% of the total mixture) was also observed. ^{31}P NMR ($CDCl_3$, ppm): 123.89. Anal. Calcd for $C_{13}H_{21}N_2OP$: C, 61.90; H, 8.33; N, 11.11. Found: C, 62.89; H, 8.73; N, 9.94.[17]

2,2-(9,10-Phenanthrenediyldioxy)-2-(2,6-dimethylphenoxy)-1,3-dimethyl-1,3,2-diazaphosphorinane, ($C_{14}H_8O_2$)(Xyl–O)P($C_3H_6Me_2N_2$) (3). Phenanthrenequinone (1.19 g, 5.71 mmol) was added to 2-(2,6-dimethylphenoxy)-1,3-dimethyl-1,3,2-diazaphosphorinane (**9**) (1.44 g, 5.71 mmol). After ca. 30 s, the mixture was dissolved in freshly distilled dichloromethane (35 °C), some insoluble product (**3**) (1.30 g) was filtered out under a nitrogen atmosphere, and the filtrate was left unperturbed. Compound **3** was obtained within 12 h as rectangular thick platelike crystals (1.00 g). Overall yield: 2.30 g, 87%. The compound was slightly soluble in dichloromethane and chloroform. Keeping **3** in solution for periods more than 18 h resulted in decomposition; mp 226–230 °C dec. ^{1}H NMR ($CDCl_3$, ppm): 1.99 (sym m, 2 H, CCH_2), 2.14 (d, J = 1.2 Hz, 6 H, CCH_3), 2.98, 2.92 (two singlets or a doublet at 2.95 ppm with $^3J(P–H)$ = 11.5 Hz, 6 H, $N(CH_3)$), 3.32 (sym m, 4 H, NCH_2), 6.60–6.80 (m, 3 H, H(Ar)), 7.40–7.70 (m, 6 H, H(Ar)), 8.55–8.65 (m, 2 H, H(Ar)). ^{31}P NMR ($CDCl_3$, ppm): −38.91. Anal. Calcd for $C_{27}H_{29}N_2O_3P$: C, 70.43; H, 6.30; N, 6.09. Found: C, 70.54; H, 6.34; N, 6.18.

(14) (a) Riddick, J. A.; Bunger, W. B., Eds. Organic Solvents. In *Physical Methods in Organic Chemistry*; Weissberger, Wiley Interscience: New York, 1970; Vol. II. (b) Vogel, A. I. *Textbook of Practical Organic Chemistry*; Lingman: London, 1978. (c) Emsley, J.; Hall, D. *The Chemistry of Phosphorus*; Wiley: New York, 1976; p 82.

(15) (a) Zwierzak, A. *Can. J. Chem.* **1967**, *45*, 2501. (b) Lucas, H. J.; Mitchell, F. W., Jr.; Scully, C. N. *J. Am. Chem. Soc.* **1950**, *72*, 5491.

(16) Hutchins, R. O.; Maryanoff, B. E.; Albrand, J. P.; Cogne, A.; Gragnaire, D.; Robert, J. B. *J. Am. Chem. Soc.* **1972**, *94*, 9151.

(17) The low nitrogen and high carbon content indicated traces of 2,6-dimethylphenol as an impurity. The ^{1}H NMR spectrum also indicated this to the extent of ~5%.

Compound 10. *trans*-2-hydroxycyclopentanemethanol (prepared according to Penney and Belleau[18]) (7.4 g, 64 mmol) in dichloromethane (30 mL) was added dropwise over a period of $^1/_2$ h to a solution of phosphorus trichloride (9.2 g, 67 mmol) in dichloromethane (100 mL) at 20 °C accompanied by a vigorous flow of dry nitrogen. The mixture was stirred at 20 °C for 14 h. The solvent was distilled at atmospheric pressure and the residue distilled in vacuo to give **10** as an oil (4.0 g, 35%), bp 82 °C/0.4–0.5 mm. ^{1}H NMR ($CDCl_3$, ppm): 1.00–6.00 (br m). ^{31}P NMR ($CDCl_3$, ppm): 145.63.

Compound 11. This phosphite was prepared by reacting **10** (3.48 g, 19.3 mmol) with 2,6-dimethylphenol (2.36 g, 19.3 mmol) in the presence of triethylamine (2.16 g, 21.4 mmol) with diethyl ether (120 mL) as the solvent at 20 °C. An oil resulted (**11**), bp 155 °C/0.4–0.5 mm (2.6 g, 50%). ^{1}H NMR ($CDCl_3$, ppm): 1.00–2.60 (m, ca. 13 H, CH_3, CH_2, CH), 3.60–5.50 (m, ca. 3 H, OCH, OCH_2), 6.60–7.20 (3, H, H(Ar)). ^{31}P NMR ($CDCl_3$, ppm): 125.24 (3), 120.46 (2). Anal. Calcd for $C_{14}H_{19}O_3P$: C, 63.16; H, 7.14. Found: C, 62.92; H, 6.91.

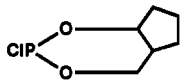

trans-fused **10**

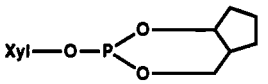

trans-fused **11**

3,3-(9,10-Phenanthrenediyldioxy)-3-(2,6-dimethylphenoxy)-2,4-dioxa-3-phosphabicyclo[4.3.0]nonane, $(C_{14}H_8O_2)(Xyl\text{–}O)P(C_5H_8CH_2O_2)$ (4). The phosphite **11** (1.11 g, 4.2 mmol) and phenanthrenequinone (0.85 g, 4.1 mmol) were heated together at 145 °C for 10 min and then cooled. The ^{31}P NMR spectrum of the mixture gave mainly two phosphorane signals, at −48.31 and −49.01 ppm (C_6D_6), in the ratio of 2:3, respectively. Crystallization from diethyl ether was repeated three times and afforded **4** with δ(P) = −49.01 ppm in a pure state (0.15 g, 8%), mp 140–160 °C. The remaining material was hydrolyzed in the process of crystallization. ^{1}H NMR (C_6D_6, ppm): 0.60–2.05 (br m, ca. 7 H, CH_2, CH), 2.43 (d, J = 1.4 Hz, 6 H, CH_3), 3.56 (td, 1 H, $^3J(H\text{–}H)$ = 10.5 Hz, $^3J(P\text{–}H)$ = 27.8 Hz, OCH), 4.25 (br m, 1 H, OCH_2), 4.60 (m, 1 H, OCH_2), 6.60–8.60 (m, 11 H, H(Ar)). Anal. Calcd for $C_{28}H_{27}O_5P$: C, 70.89; H, 5.70. Found: C, 70.80; H, 5.96.

(9,10-Phenanthrenediyldioxy)((2,2-dimethyl-1,3-propanediyl)dioxy)-phenylphosphorane, $(C_{14}H_8O_2)(Me_2C_3H_4O_2)P(Ph)$ (5). Phosphorane **5** was prepared by heating together 2-phenyl-5,5-dimethyl-1,3,2-dioxaphosphorinane (1.23 g, 5.88 mmol) and phenanthrenequinone (1.22 g, 5.88 mmol) (at 140 °C for 6 min), mp 95–100 °C. It was characterized by its ^{1}H and ^{31}P NMR spectra. ^{1}H NMR ($CDCl_3$, ppm): 0.91 (s, 3 H, $CH_2C(CH_3)_2$), 0.98 (s, 3 H, $CH_2C(CH_3)_2$), 4.04 (dd, $^3J(P\text{–}H_B)$ = 13.8 Hz, $^2J(H_A\text{–}H_B)$ = 10.8 Hz, 2 H, OCH_2(B)), 4.10 (dd, $^3J(P\text{–}H_A)$ = 19.0 Hz, $^2J(H_A\text{–}H_B)$ = 10.8 Hz, 2 H, OCH_2(A)), 7.20–8.70 (m, 13 H, H(Ar)), ^{31}P NMR ($CDCl_3$, ppm): −28.36.

The ^{1}H NMR spectrum was recorded in the range −95 to +100 °C. No significant changes were observed over this temperature range except that the fine structure in the spectrum was lost at the lower temperatures.

Other Phosphoranes. (a) (2,6-Dimethylphenoxy)((2,2-dimethyl-1,3-propanediyl)dioxy)deoxythymidine-3′,5′-diylphosphorane, $(Me_2C_3H_4O_2)(Xyl\text{–}O)P(O_3C_5H_7Thy)$ (**6**), resulted from the reaction between 2-(2,6-dimethylphenoxy)-5,5-dimethyl-1,3,2-dioxaphosphorinane and thymidine in pyridine (or a pyridine–dichloromethane mixture) in the presence of *N*-chlorodiisopropylamine. It was not isolated and could only be identified by its ^{31}P NMR spectrum, $\delta(^{31}P)$ = −69.0 ppm, along with a mixture of tetracoordinated products, $\delta(^{31}P)$ = −7 to −13 ppm.

(b) Phenyl((2,2-dimethyl-1,3-propanediyl)dioxy)(1,2-*O*-isopropylidene-D-xylofuranosyl)phosphorane, $(Me_2C_3H_4O_2)(Ph)P(O_2C_5H_6Me_2)$ (**7**), was prepared by the reaction of 2-phenyl-5,5-dimethyl-1,3,2-dioxaphosphorinane with 1,2-*O*-isopropylidene-D-xylofuranose in the presence of *N*-chlorodiisopropylamine. It is expected that the five-membered furan ring in **7** is cis-fused to the six-membered dioxaphosphorinane ring. The compound was pure by ^{31}P NMR spectroscopy (Et_2O) (δ = −52.32 ppm). Success was not achieved in obtaining a crystalline sample for an X-ray study.

X-ray Studies. All X-ray studies were done by using an Enraf-Nonius CAD4 diffractometer and graphite-monochromated molybdenum radiation (λ(K$\bar{\alpha}$) = 0.71073 Å) at an ambient temperature of 23 ● 2 °C. Details of the experimental procedures have been described previously.[19]

Crystals were mounted in thin-walled glass capillaries, which were sealed as a precaution against moisture sensitivity. Data were collected by using the θ–2θ scan mode, with $3° \le 2\theta(\text{Mo K}\bar{\alpha}) \le 50°$. The structures were solved by use of direct methods and difference Fourier techniques and were refined by full-matrix least squares.[20]

All computations were performed on a Microvax II computer using the Enraf-Nonius SDP system of programs.

X-ray Study for $(C_{14}H_8O_2)(Xyl\text{–}O)P(Me_2C_3H_4O_2)$ (1). The pale brown crystal used for the X-ray study was cut from a larger tabular crystal and was irregular with approximate dimensions of 0.30 × 0.35 × 0.45 mm.

Crystal Data: $C_{27}H_{27}O_5P$ (**1**), orthorhombic space group $P2_12_12_1$ (D_2^4-No. 19),[21] a = 7.769 (2) Å, b = 10.191 (2) Å, c = 29.594 (5) Å, Z = 4, and μ(Mo K$\bar{\alpha}$) = 1.472 cm^{-1}. A total of 2380 independent reflections ($+h,+k,+l$) were collected. An empirical absorption corrected based on ψ scans were applied (relative transmission factors from 0.969 to 1.00 on I).

The 33 independent non-hydrogen atoms were refined anisotropically. The 27 independent hydrogen atoms were included in the refinement as fixed isotropic scatterers (ideal positions or regularized difference Fourier positions for the methyl hydrogen atoms of the xylyl group). The final agreement factors[22] were R = 0.037 and R_w = 0.051 for the 1680 reflections with $I \ge 3\sigma_I$.

X-ray Study for $(C_{14}H_8O_2)(Xyl\text{–}S)P(Me_2C_3H_4O_2)$ (2). Colorless crystals of **2** either have a chunky polyfaceted appearance and are not single or form as single-crystalline plates. The crystal used for the X-ray study was an elongated plate with dimensions of 0.15 × 0.38 × 0.60 mm.

Crystal Data: $C_{27}H_{27}O_4SP$ (**2**), orthorhombic space group $P2_12_12_1$, a = 7.696 (1) Å, b = 10.441 (2) Å, c = 30.130 (6) Å, Z = 4, and μ(Mo K$\bar{\alpha}$) = 2.221 cm^{-1}. A total of 2464 independent reflections ($+h,+k,+l$) were measured. An empirical absorption corrected based on ψ scans was applied (relative transmission factors from 0.963 to 1.00 on I). The 33 independent nonhydrogen atoms were refined anisotropically. Hydrogen atoms were treated as described for **1**. The final agreement factors were R = 0.036 and R_w = 0.045 for the 1725 reflections having $I \ge 3\sigma_I$.

X-ray Study for $(C_{14}H_8O_2)(Xyl\text{–}O)P(C_3H_6Me_2N_2)$ (3). Colorless crystals of **3** are fused clusters of thick plates. The crystal used for the study was cut to approximate dimensions of 0.18 × 0.43 × 0.45 mm.

Crystal Data: $C_{27}H_{29}O_3N_2P$ (**3**), triclinic space group $P\bar{1}$ (C_i^1-No. 2),[23] a = 10.078 (3) Å, b = 10.133 (3) Å, c = 12.253 (3) Å, α = 101.60 (2)°, β = 92.81 (2)°, γ = 105.00 (2)°, Z = 2, and μ(Mo K$\bar{\alpha}$) = 1.426 cm^{-1}. A total of 4107 independent reflections ($+h,\pm k,\pm l$) were measured. An empirical absorption correction based on ψ scans was applied (relative transmission factors from 0.947 to 1.00 on I).

The 33 independent nonhydrogen atoms were refined anisotropically. The 29 independent hydrogen atoms were treated as described for **1**, except that the N–Me hydrogen atom positions were also regularized difference Fourier positions. The final agreement factors were R = 0.040 and R_w = 0.061 for the 3134 reflections having $I \ge 3\sigma_I$.

X-ray Study for $(C_{14}H_8O_2)(Xyl\text{–}O)P(C_5H_8CH_2O_2)$ (4). Colorless crystals of **4** are laths with internal defects. The crystal used for the X-ray study was cut from the center of a long lath and had dimensions of 0.20 × 0.25 × 0.50 mm.

Crystal Data: $C_{28}H_{27}O_5P$ (**4**), monoclinic space group $P2_1/c$ (C_{2h}^5-No. 14),[24] a = 15.147 (3) Å, b = 9.092 (2) Å, c = 18.089 (4) Å, β = 108.92 (2)°, Z = 4, and μ(Mo K$\bar{\alpha}$) = 1.481 cm^{-1}. A total of 4117 independent reflections ($+h,+k,\pm l$) were measured. No corrections were made for absorption.

The 34 independent non-hydrogen atoms were refined anisotropically. The 27 independent hydrogen atoms were treated as described for **1**. The final agreement factors were R = 0.040 and R_w = 0.048 for the 2099 reflections having $I \ge 3\sigma_I$.

Results

The atom-labeling scheme for **1** is shown in the ORTEP plot of Figure 1, while selected bond lengths and angles are given in Table I. The corresponding materials for **2–4** are given in Figures 3, 5, 7 and in Tables II–IV. Atomic coordinates are given in Tables V–VIII. Anisotropic thermal parameters, complete tables of bond lengths and angles, and hydrogen atom parameters are provided as supplementary material.

Discussion

Synthesis and Basic Structures. The general synthetic approach for **1–5** consisted of heating a mixture of a cyclic phosphite with phenanthrenequinone for a few minutes in the absence of solvent, followed by the addition of solvent and slow evaporation to form

(18) Penney, C. L.; Belleua, B. *Can. J. Chem.* **1978**, *56*, 2396.
(19) Sau, A. C.; Day, R. O.; Holmes, R. R. *Inorg. Chem.* **1981**, *20*, 3076.
(20) The function minimized was $\sum w(|F_o| - |F_c|)^2$, where $w^{1/2} = 2F_oLp/\sigma_I$.
(21) *International Tables for X-ray Crystallograph*; Kynoch: Birmingham, England, 1969; Vol. I, p 105.
(22) $R = \sum||F_o| - |F_c||/\sum|F_o|$, and $R_w = \{\sum w(|F_o| - |F_c|)^2/\sum w|F_o|^2\}^{1/2}$.
(23) Reference 21, p 75.
(24) Reference 21, p 99.

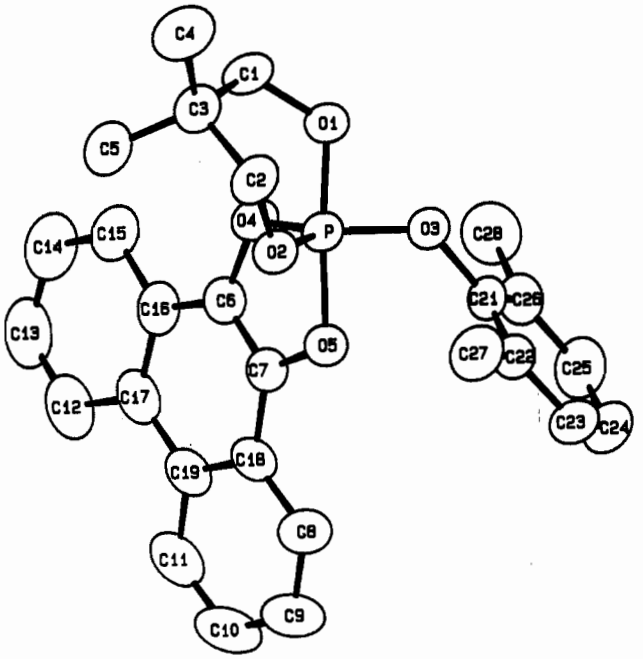

Figure 1. ORTEP plot of $(C_{14}H_8O_2)(Xyl–O)P(Me_2C_3H_4O_2)$ (**1**) with thermal ellipsoids at the 50% probability level. Hydrogen atoms are omitted for clarity.

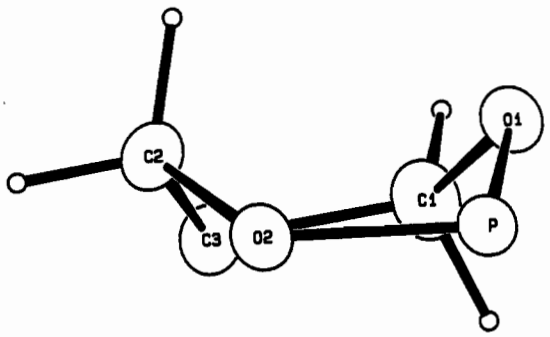

Figure 2. ORTEP plot showing the boat conformation for the six-membered phosphorinane ring in **1**.

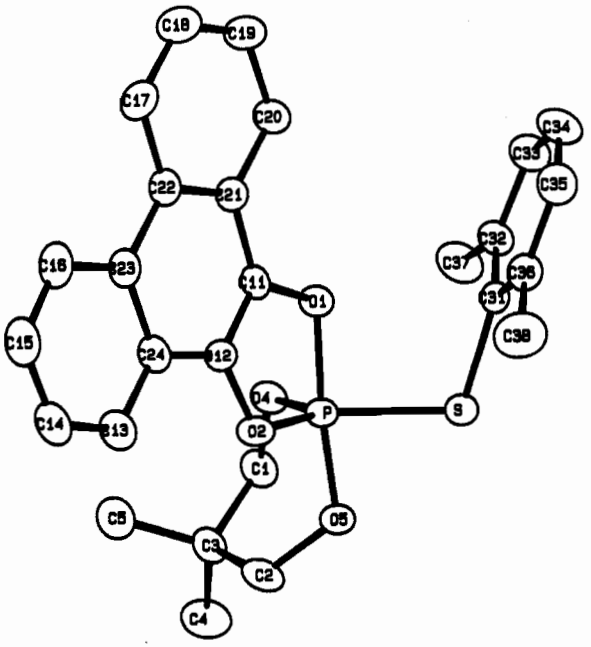

Figure 3. ORTEP plot of $(C_{14}H_8O_2)(Xyl–S)P(Me_2C_3H_4O_2)$ (**2**) with thermal ellipsoids at the 30% probability level. Hydrogen atoms are omitted for clarity.

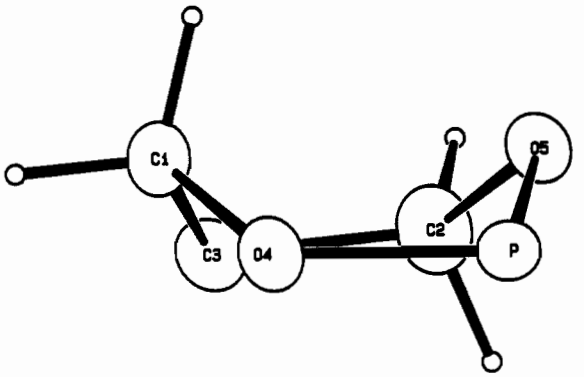

Figure 4. ORTEP plot showing the boat conformation for the six-membered phosphorinane ring in **2**.

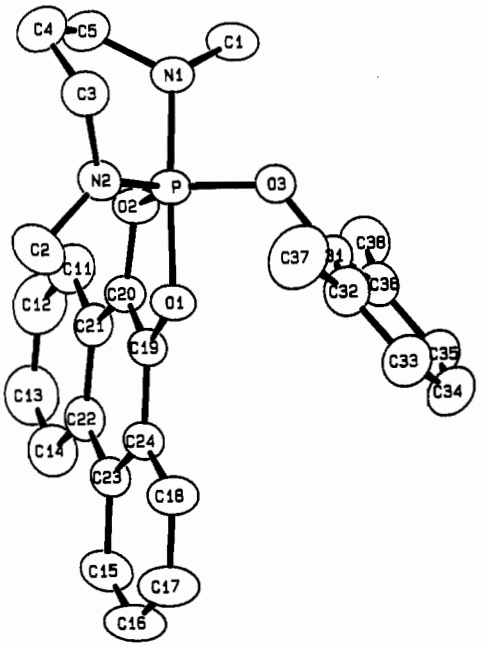

Figure 5. ORTEP plot of $(C_{14}H_8O_2)(Xyl–O)P(C_3H_6Me_2N_2)$ (**3**) with thermal ellipsoids at the 50% probability level. Hydrogen atoms are omitted for clarity.

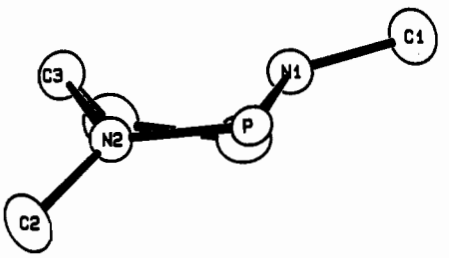

Figure 6. ORTEP plot showing the somewhat twisted boat conformation for the six-membered phosphorinane ring in **3**.

the crystalline product. The synthesis is illustrated for the formation of **1** in eq 2. Yields varied from 46 to 87% for **1–3**, but the yield was only 8% for the trans-fused phosphorinane derivative, **4**.

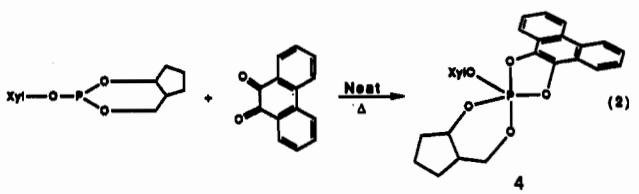

4

The molecular geometry about the phosphorus atom for all four cyclic phosphoranes, **1–4**, can be referred to a trigonal bipyramid

Table I. Selected Distances (Å) and Angles (deg) for $(C_{14}H_8O_2)(Xyl\text{-}O)P(Me_2C_3H_4O_2)$ (**1**)[a]

	Distances		
P–O1	1.637 (3)	O5–C7	1.355 (4)
P–O2	1.587 (3)	C1–C3	1.549 (6)
P–O3	1.606 (3)	C2–C3	1.525 (6)
P–O4	1.644 (3)	C3–C4	1.528 (6)
P–O5	1.723 (3)	C3–C5	1.528 (6)
O1–C1	1.431 (5)	C6–C7	1.333 (5)
O2–C2	1.448 (5)	C6–C16	1.419 (5)
O3–C21	1.408 (4)	C7–C18	1.424 (5)
O4–C6	1.388 (4)		
	Angles		
O1–P–O2	97.4 (1)	O1–C1–C3	112.8 (3)
O1–P–O3	86.1 (1)	O2–C2–C3	112.0 (3)
O1–P–O4	89.0 (1)	C1–C3–C2	107.2 (3)
O1–P–O5	173.8 (1)	C1–C3–C4	109.6 (3)
O2–P–O3	117.0 (1)	C1–C3–C5	111.6 (3)
O2–P–O4	115.1 (1)	C2–C3–C4	108.9 (3)
O2–P–O5	88.7 (1)	C2–C3–C5	109.8 (3)
O3–P–O4	127.9 (1)	C4–C3–C5	109.6 (4)
O3–P–O5	90.0 (1)	O4–C6–C7	111.6 (3)
O4–P–O5	89.6 (1)	O4–C6–C16	124.6 (3)
P–O1–C1	120.1 (2)	C7–C6–C16	123.8 (4)
P–O2–C2	120.6 (2)	O5–C7–C6	112.9 (3)
P–O3–C21	127.1 (2)	O5–C7–C18	124.3 (3)
P–O4–C6	113.4 (2)	C6–C7–C18	122.7 (3)
P–O5–C7	111.6 (2)		

[a] Estimated standard deviations are in parentheses. The atom-labeling scheme is shown in Figure 1.

Table II. Selected Distances (Å) and Angles (deg) for $(C_{14}H_8O_2)(Xyl\text{-}S)P(Me_2C_3H_4O_2)$ (**2**)[a]

	Distances		
S–P	2.098 (2)	O5–C2	1.441 (6)
S–C31	1.792 (4)	C1–C3	1.528 (6)
P–O1	1.720 (3)	C2–C3	1.515 (7)
P–O2	1.643 (3)	C3–C4	1.530 (7)
P–O4	1.589 (3)	C3–C5	1.515 (8)
P–O5	1.649 (3)	C11–C12	1.338 (6)
O1–C11	1.365 (5)	C11–C21	1.417 (6)
O2–C12	1.389 (5)	C12–C24	1.416 (6)
O4–C1	1.455 (5)		
	Angles		
P–S–C31	107.4 (1)	O4–C1–C3	110.5 (3)
S–P–O1	91.4 (1)	O5–C2–C3	114.4 (4)
S–P–O2	127.0 (1)	C1–C3–C2	107.3 (4)
S–P–O4	119.4 (1)	C1–C3–C4	107.7 (4)
S–P–O5	83.0 (1)	C1–C3–C5	110.5 (4)
O1–P–O2	90.4 (1)	C2–C3–C4	109.8 (4)
O1–P–O4	89.1 (1)	C2–C3–C5	111.2 (4)
O1–P–O5	173.0 (2)	C4–C3–C5	110.1 (4)
O2–P–O4	113.6 (2)	O1–C11–C12	112.8 (3)
O2–P–O5	89.6 (1)	O1–C11–C21	124.7 (4)
O4–P–O5	97.3 (2)	C12–C11–C21	122.6 (4)
P–O1–C11	111.1 (2)	O2–C12–C11	112.0 (3)
P–O2–C12	113.0 (2)	O2–C12–C24	123.8 (3)
P–O4–C1	120.6 (3)	C11–C12–C24	124.1 (4)
P–O5–C2	119.7 (3)		

[a] Estimated standard deviations are in parentheses. The atom-labeling scheme is shown in Figure 3.

(TBP) with the ring systems spanning axial–equatorial sites and the acyclic substituents in an equatorial position. The six-membered rings are in a boat or twisted-boat conformation in each case with the axial oxygen atom (or nitrogen atom in the case of **3**) at the prow and the opposing carbon atom at the stern. This is illustrated for the pentaoxyphosphorane **1** in Figure 2, which shows the axial oxygen atom, O1, and the carbon atom, C2, occupying these positions. The four atoms forming the base of the boat, P, O2, C1, and C3, are coplanar to within ±0.049 Å. This planarity is very similar to that found for the phosphorinane ring in the cyclic phosphorane **2**. Here the four atoms forming the base of the boat (P, O4, C2, and C3) are coplanar to with ±0.037 Å. Phosphorane **2** is chemically identical with **1** except

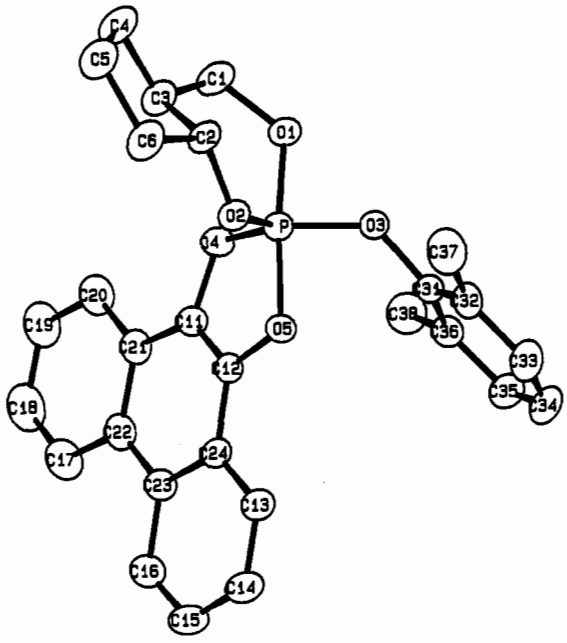

Figure 7. ORTEP plot of $(C_{14}H_8O_2)(Xyl\text{-}O)P(C_5H_8CH_2O_2)$ (**4**) with thermal ellipsoids at the 30% probability level. Hydrogen atoms are omitted for clarity.

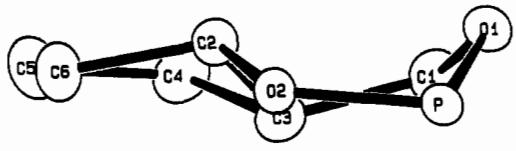

Figure 8. ORTEP plot of the fused ring system showing the twist-boat conformation for the six-membered phosphorinane ring in **4**.

Table III. Selected Distances (Å) and Angles (deg) for $(C_{14}H_8O_2)(Xyl\text{-}O)P(C_3H_6Me_2N_2)$ (**3**)[a]

	Distances		
P–O1	1.759 (1)	O3–C31	1.405 (2)
P–O2	1.677 (2)	N1–C1	1.465 (3)
P–O3	1.621 (2)	N1–C5	1.482 (3)
P–N1	1.715 (2)	N2–C2	1.466 (3)
P–N2	1.646 (2)	N2–C3	1.481 (3)
O1–C19	1.346 (3)	C3–C4	1.501 (4)
O2–C20	1.382 (2)	C4–C5	1.519 (4)
	Angles		
O1–P–O2	87.72 (7)	P–O2–C20	114.7 (1)
O1–P–O3	89.00 (7)	P–O3–C31	127.6 (1)
O1–P–N1	176.61 (8)	P–N1–C1	117.8 (1)
O1–P–N2	89.11 (8)	P–N1–C5	116.1 (1)
O2–P–O3	118.52 (8)	C1–N1–C5	111.1 (2)
O2–P–N1	90.80 (8)	P–N2–C2	125.9 (1)
O2–P–N2	120.50 (9)	P–N2–C3	119.7 (1)
O3–P–N1	89.02 (8)	C2–N2–C3	113.9 (2)
O3–P–N2	120.8 (1)	N2–C3–C4	111.2 (2)
N1–P–N2	94.27 (9)	C3–C4–C5	110.0 (2)
P–O1–C19	112.9 (1)	N1–C5–C4	110.7 (2)

[a] Estimated standard deviations are in parentheses. The atom-labeling scheme is shown in Figure 5.

that the acyclic oxygen atom, O3, in **1** has been replaced by the sulfur atom, S, in **2**. The two compounds are, in fact, isomorphous, where the approximate coordinates of the atoms in **2** can be generated from those of **1** by the operation $^1/_2 + x, y, ^1/_2 + z$. Except for the increase in the P–S bond length (2.098 (2) Å) compared to the P–O3 bond length (1.606 (3) Å), the molecular geometry in the two species is very similar. Figures 4, 6, and 8 depict the phosphorinane ring structures for the spirocyclic phosphoranes, **2**–**4**, respectively.

In a comparison of phosphorane **3** to phosphorane **1** the dioxaphosphorinane ring has been replaced by a diazaphosphorinane ring. Despite the fact that oxygen is more electronegative than

Table IV. Selected Distances (Å) and Angles (deg) for $(C_{14}H_8O_2)(Xyl\text{-}O)P(C_5H_8CH_2O_2)$ (**4**)[a]

	Distances		
P–O1	1.632 (2)	C1–C3	1.514 (5)
P–O2	1.593 (2)	C2–C3	1.495 (5)
P–O3	1.603 (2)	C2–C6	1.509 (5)
P–O4	1.643 (2)	C3–C4	1.529 (5)
P–O5	1.722 (2)	C4–C5	1.542 (7)
O1–C1	1.444 (4)	C5–C6	1.546 (6)
O2–C2	1.453 (4)	C11–C12	1.335 (5)
O3–C31	1.406 (4)	C11–C21	1.414 (4)
O4–C11	1.394 (3)	C12–C24	1.426 (4)
O5–C12	1.358 (3)		
	Angles		
O1–P–O2	98.4 (1)	O2–C2–C3	111.6 (2)
O1–P–O3	85.5 (1)	O2–C2–C6	112.9 (3)
O1–P–O4	89.4 (1)	C3–C2–C6	104.9 (3)
O1–P–O5	173.0 (1)	C1–C3–C2	109.9 (3)
O2–P–O3	117.1 (1)	C1–C3–C4	117.8 (3)
O2–P–O4	115.0 (1)	C2–C3–C4	101.9 (3)
O2–P–O5	88.3 (1)	C3–C4–C5	104.1 (3)
O3–P–O4	127.8 (1)	C4–C5–C6	106.7 (3)
O3–P–O5	89.7 (1)	C2–C6–C5	102.7 (3)
O4–P–O5	89.6 (1)	O4–C11–C12	111.1 (2)
P–O1–C1	122.8 (2)	O4–C11–C21	123.8 (3)
P–O2–C2	119.4 (2)	C12–C11–C21	125.0 (3)
P–O3–C31	129.5 (2)	O5–C12–C11	113.2 (3)
P–O4–C11	113.9 (2)	O5–C12–C24	124.9 (3)
P–O5–C12	111.7 (2)	C11–C12–C24	121.9 (3)
O1–C1–C3	109.8 (3)		

[a] Estimated standard deviations are in parentheses. The atom-labeling scheme is shown in Figure 7.

Table V. Atomic Coordinates and Thermal Parameters (Å²) in Crystalline $(C_{14}H_8O_2)(Me_2C_3H_4O_2)P(O\text{-}Xyl)$ (**1**)[a]

atom[b]	x	y	z	B_{equiv}[c]
P	0.6560 (1)	0.0759 (1)	0.34616 (3)	3.13 (2)
O1	0.5796 (3)	0.2153 (2)	0.32736 (8)	3.52 (5)
O2	0.8361 (3)	0.0815 (2)	0.32093 (8)	3.65 (5)
O3	0.4992 (3)	0.0081 (2)	0.31957 (8)	3.53 (5)
O4	0.6554 (3)	0.1373 (2)	0.39753 (8)	3.61 (5)
O5	0.7141 (3)	−0.0744 (3)	0.36797 (8)	3.75 (5)
C1	0.6767 (6)	0.3336 (4)	0.3327 (2)	4.39 (9)
C2	0.8770 (5)	0.1892 (4)	0.2909 (1)	3.91 (8)
C3	0.8629 (5)	0.3217 (4)	0.3145 (1)	3.94 (8)
C4	0.8966 (7)	0.4303 (5)	0.2801 (2)	5.9 (1)
C5	0.9954 (6)	0.3301 (4)	0.3526 (2)	5.3 (1)
C6	0.7225 (5)	0.0525 (4)	0.4297 (1)	3.44 (8)
C7	0.7504 (5)	−0.0666 (4)	0.4127 (1)	3.33 (8)
C8	0.8169 (6)	−0.3037 (4)	0.4229 (2)	4.41 (9)
C9	0.8592 (6)	−0.4048 (4)	0.4510 (2)	5.4 (1)
C10	0.8942 (6)	−0.3800 (4)	0.4969 (2)	5.7 (1)
C11	0.8855 (6)	−0.2534 (5)	0.5134 (1)	5.2 (1)
C12	0.8594 (6)	0.0188 (5)	0.5491 (1)	5.4 (1)
C13	0.8291 (6)	0.1434 (5)	0.5649 (2)	5.9 (1)
C14	0.7598 (6)	0.2410 (5)	0.5371 (2)	5.9 (1)
C15	0.7243 (6)	0.2151 (4)	0.4925 (1)	4.6 (1)
C16	0.7549 (5)	0.0868 (4)	0.4754 (1)	3.94 (8)
C17	0.8196 (5)	−0.0147 (4)	0.5035 (1)	4.22 (9)
C18	0.8040 (5)	−0.1749 (4)	0.4397 (1)	3.58 (8)
C19	0.8383 (5)	−0.1474 (4)	0.4861 (1)	3.94 (8)
C21	0.4419 (5)	−0.1224 (3)	0.3237 (1)	3.38 (7)
C22	0.5164 (5)	−0.2171 (4)	0.2962 (1)	3.66 (8)
C23	0.4517 (6)	−0.3429 (4)	0.2994 (2)	4.8 (1)
C24	0.3178 (7)	−0.3727 (4)	0.3281 (2)	5.5 (1)
C25	0.2462 (6)	−0.2762 (5)	0.3547 (2)	5.3 (1)
C26	0.3042 (5)	−0.1462 (4)	0.3520 (1)	4.15 (9)
C27	0.6655 (6)	−0.1876 (4)	0.2650 (2)	5.0 (1)
C28	0.2269 (6)	−0.0401 (5)	0.3800 (2)	5.9 (1)

[a] Numbers in parentheses are estimated standard deviations. [b] Atoms are labeled to agree with Figure 1. [c] Equivalent isotropic thermal parameters are calculated as $(4/3)[a^2\beta_{11} + b^2\beta_{22} + c^2\beta_{33} + ab(\cos\gamma)\beta_{12} + ac(\cos\beta)\beta_{13} + bc(\cos\alpha)\beta_{23}]$.

nitrogen, the ring placement remains axial–equatorial. The conformation of the diazaphosphorinane ring, while analogous

Table VI. Atomic Coordinates and Thermal Parameters (Å²) in Crystalline $(C_{14}H_8O_2)(Me_2C_3H_4O_2)P(S\text{-}Xyl)$ (**2**)[a]

atom[b]	x	y	z	B_{equiv}[c]
S	0.9172 (2)	0.0491 (1)	0.81815 (4)	3.65 (2)
P	1.1454 (2)	0.10526 (9)	0.85088 (3)	3.01 (2)
O1	1.1804 (4)	−0.0483 (2)	0.86948 (8)	3.34 (6)
O2	1.1622 (4)	0.1600 (2)	0.90181 (9)	3.59 (6)
O4	1.3256 (4)	0.0990 (3)	0.82519 (9)	3.78 (6)
O5	1.0863 (4)	0.2491 (2)	0.83396 (9)	3.53 (6)
C1	1.3745 (6)	0.1995 (4)	0.7941 (2)	4.0 (1)
C2	1.2062 (8)	0.3545 4)	0.8375 (2)	4.8 (1)
C3	1.3837 (6)	0.3289 (4)	0.8177 (2)	4.0 (1)
C4	1.4260 (9)	0.4307 (5)	0.7828 (2)	6.0 (1)
C5	1.5230 (8)	0.3269 (5)	0.8533 (2)	5.6 (1)
C11	1.2236 (6)	−0.0491 (4)	0.9134 (1)	3.09 (8)
C12	1.2143 (6)	0.0671 (4)	0.9320 (1)	3.14 (8)
C13	1.2495 (7)	0.2169 (4)	0.9958 (2)	4.3 (1)
C14	1.2966 (8)	0.2346 (5)	1.0387 (2)	5.1 (1)
C15	1.3540 (8)	0.1315 (5)	1.0644 (1)	5.1 (1)
C16	1.3653 (7)	0.0114 (5)	1.0470 (2)	4.7 (1)
C17	1.3696 (7)	−0.2507 (5)	1.0067 (2)	4.7 (1)
C18	1.3689 (8)	−0.3712 (5)	0.9878 (2)	5.4 (1)
C19	1.3204 (7)	−0.3874 (4)	0.9438 (2)	4.8 (1)
C20	1.2727 (7)	−0.2837 (4)	0.9181 (2)	4.1 (1)
C21	1.2700 (6)	−0.1601 (4)	0.9378 (1)	3.25 (9)
C22	1.3185 (6)	−0.1418 (4)	0.9827 (1)	3.63 (9)
C23	1.3148 (6)	−0.0132 (4)	1.0025 (1)	3.63 (9)
C24	1.2591 (6)	0.0934 (4)	0.9767 (1)	3.63 (9)
C31	0.8924 (5)	−0.1200 (4)	0.8264 (1)	3.23 (8)
C32	0.9859 (7)	−0.2053 (4)	0.7992 (1)	3.8 (1)
C33	0.9505 (8)	−0.3348 (4)	0.8038 (2)	4.9 (1)
C34	0.8331 (8)	−0.3780 (4)	0.8340 (2)	5.6 (1)
C35	0.7451 (7)	−0.2947 (5)	0.8610 (2)	5.3 (1)
C36	0.7715 (6)	−0.1614 (4)	0.8577 (2)	4.0 (1)
C37	1.1223 (8)	−0.1627 (5)	0.7670 (2)	5.3 (1)
C38	0.6771 (8)	−0.0692 (6)	0.8882 (2)	6.7 (1)

[a] Numbers in parentheses are estimated standard deviations. [b] Atoms are labeled to agree with Figure 3. [c] See footnote *c* of Table V.

Table VII. Atomic Coordinates and Thermal Parameters (Å²) in Crystalline $(C_{14}H_8O_2)(C_3H_6Me_2N_2)P(O\text{-}Xyl)$ (**3**)[a]

atom[b]	x	y	z	B_{equiv}[c]
P	0.19327 (5)	0.34620 (5)	0.35530 (4)	2.60 (1)
O1	0.0547 (1)	0.1944 (1)	0.3393 (1)	2.84 (3)
O2	0.0923 (1)	0.4084 (1)	0.2778 (1)	2.98 (3)
O3	0.2848 (1)	0.2505 (1)	0.2917 (1)	2.94 (3)
N1	0.3288 (2)	0.4918 (2)	0.3625 (2)	3.04 (4)
N2	0.1899 (2)	0.3716 (2)	0.4920 (2)	3.24 (4)
C1	0.3823 (3)	0.5176 (3)	0.2575 (2)	4.11 (6)
C2	0.0687 (3)	0.3238 (3)	0.5501 (2)	5.21 (7)
C3	0.3113 (2)	0.4660 (3)	0.5674 (2)	3.84 (5)
C4	0.3317 (3)	0.6154 (3)	0.5584 (2)	4.82 (7)
C5	0.3181 (3)	0.6232 (2)	0.4360 (2)	3.95 (6)
C11	−0.1231 (3)	0.4791 (2)	0.1446 (2)	3.88 (5)
C12	−0.2301 (3)	0.5043 (3)	0.0850 (2)	5.06 (6)
C13	−0.3579 (3)	0.4044 (3)	0.0605 (2)	5.22 (6)
C14	−0.3800 (3)	0.2820 (3)	0.0954 (2)	4.40 (6)
C15	−0.4198 (2)	0.0098 (3)	0.1675 (2)	4.31 (6)
C16	−0.4316 (3)	−0.1149 (3)	0.1984 (2)	5.08 (7)
C17	−0.3215 (3)	−0.1399 (3)	0.2553 (2)	4.96 (6)
C18	−0.1980 (2)	−0.0372 (2)	0.2825 (2)	3.72 (5)
C19	−0.0578 (2)	0.1999 (2)	0.2784 (2)	2.63 (4)
C20	−0.0394 (2)	0.3206 (2)	0.2438 (2)	2.75 (4)
C21	−0.1441 (2)	0.3533 (2)	0.1811 (2)	2.87 (4)
C22	−0.2748 (2)	0.2504 (2)	0.1569 (2)	3.22 (5)
C23	−0.2947 (2)	0.1184 (2)	0.1924 (2)	3.08 (5)
C24	−0.1839 (2)	0.0916 (2)	0.2523 (2)	2.86 (4)
C31	0.2402 (2)	0.1082 (2)	0.2376 (2)	3.03 (4)
C32	0.2462 (3)	0.0081 (2)	0.2989 (2)	3.87 (5)
C33	0.2055 (3)	−0.1324 (3)	0.2415 (3)	4.94 (6)
C34	0.1634 (3)	−0.1685 (3)	0.1284 (3)	5.16 (7)
C35	0.1610 (3)	−0.0667 (3)	0.0698 (2)	4.57 (6)
C36	0.2002 (2)	0.0745 (2)	0.1231 (2)	3.41 (5)
C37	0.2935 (4)	0.0485 (3)	0.4228 (2)	5.86 (7)
C38	0.1995 (3)	0.1845 (3)	0.0574 (2)	4.29 (6)

[a] Numbers in parentheses are estimated standard deviations. [b] Atoms are labeled to agree with Figure 5. [c] See footnote *c* of Table V.

Table VIII. Atomic Coordinates and Thermal Parameters (Å^2) in Crystalline $(C_{14}H_8O_2)(C_5H_8CH_2O_2)P(O\text{-}Xyl)$ (**4**)[a]

atom[b]	x	y	z	B_{equiv}[c]
P	0.21219 (6)	0.0813 (1)	0.20482 (4)	3.34 (2)
O1	0.2235 (1)	0.0816 (2)	0.1181 (1)	3.96 (5)
O2	0.1171 (1)	−0.0089 (2)	0.1843 (1)	3.71 (5)
O3	0.2042 (2)	0.2565 (2)	0.1951 (1)	3.86 (5)
O4	0.3076 (1)	−0.0182 (3)	0.2372 (1)	3.71 (5)
O5	0.2099 (1)	0.0983 (2)	0.2990 (1)	3.50 (5)
C1	0.2237 (2)	−0.0516 (4)	0.0746 (2)	4.78 (9)
C2	0.0793 (2)	−0.0776 (4)	0.1080 (2)	4.09 (8)
C3	0.1528 (2)	−0.1589 (4)	0.0860 (2)	4.44 (8)
C4	0.0945 (3)	−0.2473 (4)	0.0150 (2)	5.6 (1)
C5	0.0053 (3)	−0.2867 (4)	0.0341 (2)	6.3 (1)
C6	0.0056 (3)	−0.1913 (4)	0.1049 (2)	5.5 (1)
C11	0.3324 (2)	−0.0529 (4)	0.3164 (2)	3.45 (7)
C12	0.2768 (2)	0.0148 (3)	0.3498 (2)	3.24 (7)
C13	0.2367 (2)	0.0798 (4)	0.4680 (2)	4.31 (8)
C14	0.2545 (3)	0.0672 (4)	0.5469 (2)	5.17 (9)
C15	0.3257 (3)	−0.0250 (5)	0.5905 (2)	5.6 (1)
C16	0.3805 (3)	−0.1001 (4)	0.5563 (2)	4.95 (9)
C17	0.5003 (2)	−0.2558 (4)	0.4776 (2)	5.3 (1)
C18	0.5532 (3)	−0.3255 (5)	0.4400 (2)	6.0 (1)
C19	0.5345 (2)	−0.3090 (4)	0.3603 (2)	5.6 (1)
C20	0.4631 (2)	−0.2198 (4)	0.3183 (2)	4.64 (9)
C21	0.4078 (2)	−0.1461 (4)	0.3556 (2)	3.82 (8)
C22	0.4248 (2)	−0.1631 (4)	0.4376 (2)	4.03 (8)
C23	0.3662 (2)	−0.0879 (4)	0.4750 (2)	3.88 (8)
C24	0.2912 (2)	0.0032 (3)	0.4315 (2)	3.44 (7)
C31	0.2055 (2)	0.3652 (4)	0.2508 (2)	3.74 (7)
C32	0.1209 (2)	0.4280 (4)	0.2468 (2)	4.40 (8)
C33	0.1246 (3)	0.5436 (4)	0.2983 (2)	5.9 (1)
C34	0.2079 (3)	0.5922 (4)	0.3501 (2)	6.4 (1)
C35	0.2901 (3)	0.5260 (4)	0.3515 (2)	5.6 (1)
C36	0.2911 (2)	0.4109 (4)	0.3009 (2)	4.31 (8)
C37	0.0301 (3)	0.3759 (5)	0.1902 (2)	6.4 (1)
C38	0.3805 (3)	0.3423 (5)	0.3000 (2)	5.7 (1)

[a] Numbers in parentheses are estimated standard deviations. [b] Atoms are labeled to agree with Figure 7. [c] See footnote *c* of Table V.

to that of the dioxa derivatives **1** and **2**, exhibits a slightly twisted boat (Figure 6), where the four atoms forming the base of the boat (P, N2, C4, and C5) are copolanar to within ±0.087 Å.

The geometry at the equatorial nitrogen atom, N2, is essentially planar, with atoms N2, P, C2, and C3 coplanar to within ±0.033 Å. Alternatively, the sum of the angles about N2 is 359.5 (4)°. In contrast, the geometry at the axial N1 is more pyramidal with atom N1 displaced by 0.352 Å out of the plane defined by P, C1, and C5. Alternatively, the sum of the angles about N1 is 345.0 (4)°.

The pentaoxy derivative **4** differs from **1** only in the replacement of the phosphorinane ring methyl substituents by a trans-fused cyclopentane ring. This compositional change has only a modest effect on the molecular geometry of **4** compared to **1**. For example, the boat conformation for **1** (Figure 2) becomes somewhat twisted (Figure 8). The atoms forming the base of the boat for **4** (P, C1, C3, and O2) are accordingly less coplanar with deviations from coplanarity of ±0.138 Å.

The conformation of the fused five-membered ring can be viewed as a slightly twisted envelope, with C2 as a flap atom. The atoms C3, C4, C5, and C6 are coplanar to within ±0.075 Å, with C2 displaced out of this plane by 0.613 Å. Alternatively, C2 and C3 are displaced in opposite directions from the plane defined by C4, C5, and C6 by distances of 0.364 and 0.324 Å, respectively.

The structure of **4** represents one of three known examples of a fused five-membered-ring system in a pentaoxyphosphorane.[34] It differs from a phosphorane intermediate proposed for phosphodiesterase action on c-AMP on the basis of semiempirical CNDO/2 calculations,[9] which place the 3′-oxygen atom at the apical position (depicted in the Introduction). This would correspond to the attachment of the fused cyclopentane ring in **4** to the phosphorinane ring carbon atoms C1 and C3 (Figure 7). The preference in **4** to attachment of the five-membered ring at C2 and C3 may be governed by a more conformationally stable fused-ring system that results when the stern atom of the phosphorinane boat conformation, C2, is common to both rings in the trans-fused system. Alternatively, a greater electronegatively effect is provided at the apical oxygen atom by the annelation of the cyclopentane ring as observed for **4** compared to attachment at C1 and C3.

Table IX. Dihedral Angles between P–O_{eq}–C Bonds and Equatorial Planes for Phosphoranes (deg)

	ring size, no. of atoms		
	5	6	xylyloxy group
1	80.2	86.2	82.6
2	88.6	80.3	87.6
3	88.8	71.1	81.3
4	82.4	83.4	85.4
av	85.0	80.2	84.2

With regard to the disposition of the dioxyphenanthrene ligand in all four cyclic phosphoranes **1**–**4**, the phosphorus atoms lie essentially in the plane, resulting in nearly planar five-membered rings. For **1**, the atoms P, O4, O5, C6, and C7 are coplanar to within ±0.055 Å; for **2**, the atoms P, O1, O2, C11, and C12 are coplanar to within ±0.045 Å; for **3**, the atoms P, O1, O2, C19, and C20 are coplanar to within ±0.008 Å; and for **4**, the atoms P, O4, O5, C11, and C12 are coplanar to within ±0.041 Å.

In line with Trippett's conclusion[6] that the boat form in an apical–equatorial orientation of a TBP is the only one that allows the lone pair on the equatorial atom of the phosphorinane ring bonded to phosphorus to approach the equatorial plane, the dihedral angles between the endocyclic P–O_{eq}–C bonds and equatorial planes for **1**–**4** are not too far from the 90° angle that would maximize this effect. As indicated in Table IX, a range of 71 to 86° is found for these phosphoranes. The average value for this angle is 80.2° and compares with an average value of 84.2° for the acyclic xylyloxy group whose rotation is not inhibited by ring constraints. These dihedral angles compare with those found from X-ray structures[4] on related spirocyclic pentaoxyphosphoranes, F–I, which contain phosphorinane rings in boat conformations. Here, the average dihedral angle between the P–O_{eq}–C ring bond and the equatorial plane for the six-membered ring is 80.4 and 82.8° for the xylyloxy group.

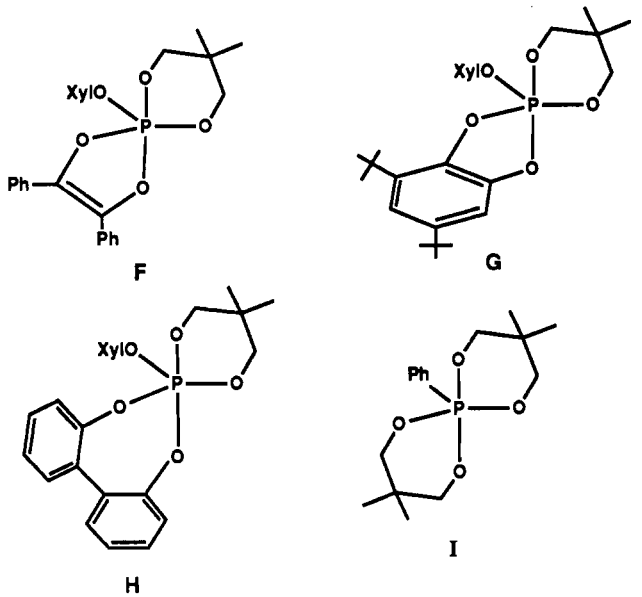

A comparison of the bond lengths and angles at phosphorus for the phosphoranes, **1**–**4**, reveals certain trends. The largest apical–equatorial bond angle is all cases occurs in the phosphorinane rings. For the oxaphosphorinanes, **1**, **2**, and **4**, this angle ranges from 97.3 (2) to 98.4 (1)°, while for the azaphosphorinane, **3**, this angle is 94.27 (9)°. This is similar to the respective angles in the phosphorinane rings of F–I,[4] which cover the range from 92.6 to 96.7°. For the five-membered ring formed by the di-

Table X. P–O Bond Distances in Spirocyclic Phosphoranes (Å)

	five-membered ring		six-membered ring		xylyloxy group
compd[a]	P–O_{eq}	P–O_{ap}	P–O_{eq}	P–O_{ap}	P–O_{eq}
1	1.644 (3)	1.723 (3)	1.587 (3)	1.637 (3)	1.606 (3)
2	1.643 (3)	1.720 (3)	1.589 (3)	1.649 (3)	
3	1.677 (2)	1.759 (1)			1.621 (2)
4	1.643 (2)	1.722 (2)	1.593 (2)	1.632 (2)	1.603 (2)
EA[b]	1.649 (3)	1.746 (2)			1.607 (3)
EB[b]	1.645 (2)	1.753 (2)			1.598 (2)
F	1.629 (2)	1.707 (2)	1.595 (2)	1.635 (2)	1.599 (2)
G	1.628 (9)	1.713 (9)	1.587 (9)	1.634 (9)	1.598 (9)
H			1.590 (4)	1.634 (3)	1.604 (3)
IA[c]			1.618 (5)	1.681 (5)	
IB[c]			1.624 (5)	1.682 (5)	
av	1.645 (3)	1.730 (3)	1.598 (4)	1.648 (4)	1.605 (3)

[a] Entries for 1–4 are from this work; entries for E are from ref 3; entries for F–I are from ref 4. [b] A represent data for a triclinic form of E. B refers to a monoclinic form of E. [c] Two sets of positions were obtained for the ring oxygen atoms that were refined in half-occupancy.

oxyphenanthrene ligand in **1**–**4**, the O_{ap}–P–O_{eq} angle ranges from 87.7 to 90.4° with the average for the O_{ap}–P–O_{eq} angles in the five-membered rings of **1**–**4** (89.3°) being 8.4° smaller than the average for the corresponding angle in the six-membered ring (97.7°)

There is the usual tendency for bonds to apical ligands to be longer than bonds to equatorial ligands.[25,26] This trend is strictly followed in comparing bonds that are chemically similar. Ligation to the dioxyphenanthrene ligand results in longer P–O bond lengths (Table X). The longest P–O bond in all four compounds is found in the P–O_{ap} bond to this ligand, with bond lengths that range from 1.720 (3) to 1.723 (3) Å for the oxaphosphorinane compounds, **1**, **2**, and **4**. For the azaphosphorinane, where the P–O bond lengths tend to be longer, this bond length is 1.759 (1) Å. The longest P–O_{eq} bond length in all four compounds also involves this ligand. For the oxaphosphorinanes, this P–O bond length ranges from 1.643 (3) to 1.644 (3) Å and for the azaphosphorinane has a value of 1.677 (2) Å.

For compounds **1**, **2**, and **4** the shortest P–O bond is the equatorial bond involving the phosphorinane ring, with bond lengths that range from 1.587 (3) to 1.593 (2) Å.

The average values for the various P–O bond lengths listed in Table X for the phosphoranes **1**–**4** and E–I emphasize the differences between the five- and six-membered rings, showing about a 0.05-Å increase for the P–O_{eq} bond and a 0.08-Å increase for the P–O_{ap} bond on going from the six-membered to the five-membered rings. This is in line with the expected greater ring strain associated with planar unsaturated five-membered rings found in apical–equatorial positions of **1**–**4** and E–G[3,4] compared to the boat conformations of saturated six-membered rings in **1**, **2**, **4**, and F–I.[4] The average P–O_{eq} bond length for the six-membered ring, which is not significantly different from the average P–O_{eq} bond length for the acyclic xylyloxy group, suggests an absence of any substantial ring strain for the boat form of this ring.

Structural Distortions. For compounds **1**, **2**, and **4** distortions away from the ideal TBP geometry lie on the Berry pseudorotation coordinate[27] connecting the TBP with a rectangular pyramid (RP), where the equatorial oxygen atom of the six-membered ring in the TBP is the pivotal atom in the pseudorotation process. By use of the dihedral angle method with unit vectors to assess displacement,[28] **1** is displaced 22.1% from the TBP toward the RP. For **2** and **4** these values are 20.2% and 22.5%, respectively. The ease of distortion of the TBP in this way is related to the fluxional nature of these phosphoranes demonstrated by ^{1}H NMR spectra discussed in the next section. For compound **3**, the equatorial nitrogen atom can be viewed as the pivotal atom in distortions away from the TBP geometry, but the Berry pseudorotation coordinate is not followed. Rather in this case as the N1–P–O1 angle closes down from the ideal 180° to the observed 176.61 (8)°, the O2–P–O3 angle also closes down from the ideal 120° to the observed 118.52 (8)°.

NMR and Intramolecular Ligand Exchange. For all of the spirocyclic phosphoranes **1**–**5** like E[3] discussed earlier, the ^{1}H NMR data at room temperature are consistent with the presence of TBP ground-state structures having rings positioned in apical–equatorial sites undergoing intramolecular ligand exchange by a simple Berry process.[27] This process is depicted in the following labeled schematic:

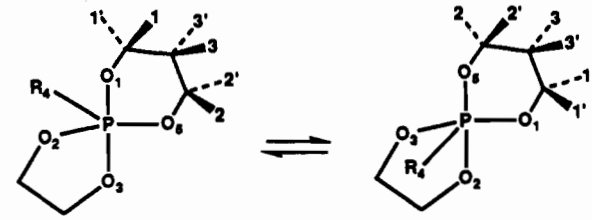

This process leads to two types of methylene ring protons for the phosphorinane ring and two kinds of phosphorinane ring methyl substituents that are present in **1** and **2**. Of these five derivatives, all of which contain the dioxyphenanthrene ligand, only the ^{1}H NMR data for the sulfur-containing phosphorane, **2**, show a higher temperature exchange process that supports an intermediate with diequatorial ring placement, J.

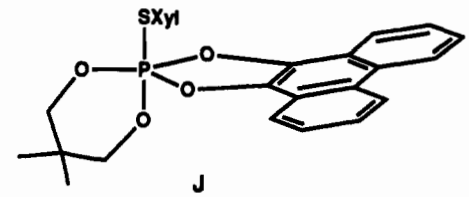

J

Variable-temperature ^{1}H NMR spectra attributable to the methylene group of the six-membered ring are compared in Figure 9 for phosphoranes **1** and **2**, which differ only in the type of xylyl group attached to phosphorus. Figure 10 contrasts the full ^{1}H NMR spectra of **1** and **2** at 23 and –95 °C. The sulfur-containing derivative, **2**, exhibits more fluxional character than the xylyloxy derivative, **1**. The multiplet pattern at lower temperatures resolves into a simple doublet above 41 °C for **2**, indicating the presence of only one type of methylene proton. The doublet is due to ^3J phosphorus coupling and indicates the exchange process is intramolecular. Ligand exchange via J with the dioxyphenanthrene ring system located diequatorially will equilibrate the methylene protons that reside on opposite sides of the six-membered ring. Exchange via intermediates with the phosphorinane ring in a diequatorial location will not equilibrate these methylene protons, although this process probably is occurring at the higher temperatures, since the spirocyclic I[4] containing two such rings shows equivalence of all methylene protons at 0 °C.

The OCH_2 multiplets for **1** and **2** have been analyzed (see Experimental Section) in terms of an ABX pattern. In this region (from 91 to –95 °C for **1** and from 24 to –40 °C for **2**), two kinds of methylene protons are indicated. The two quartets for **1** are better resolved at 300 MHz (Figure 9c) compared to the 200-MHz spectrum shown in Figure 9b. The latter observation indicates the presence of a simple Berry pseudorotational process that maintains the ring systems in apical–equatorial sites of trigonal bipyramids exchanging via an intervening square pyramid. In either case, a pattern indicating the presence of four methylene protons, which is expected for a static structure, is absent even at reduced temperatures, although the ^{1}H spectrum of the sulfur derivative, **2**, appears to show the onset of coalescence in the OCH_2 region at –38 °C. However, by –95 °C, only two very broad peaks are present and not the four ABX quartets expected for a static structure.

(25) Holmes, R. R. *Pentacoordinated Phosphorus, Structure and Spectroscopy*; ACS Monograph 175; American Chemical Society: Washington, DC, 1980; Chapter 2 and references cited therein.
(26) Holmes, R. R. *Prog. Inorg. Chem.* **1984**, *32*, 119.
(27) Berry, R. S. *J. Chem. Phys.* **1960**, *32*, 933.
(28) Holmes, R. R.; Deiters, J. A. *J. Am. Chem. Soc.* **1977**, *99*, 3318.

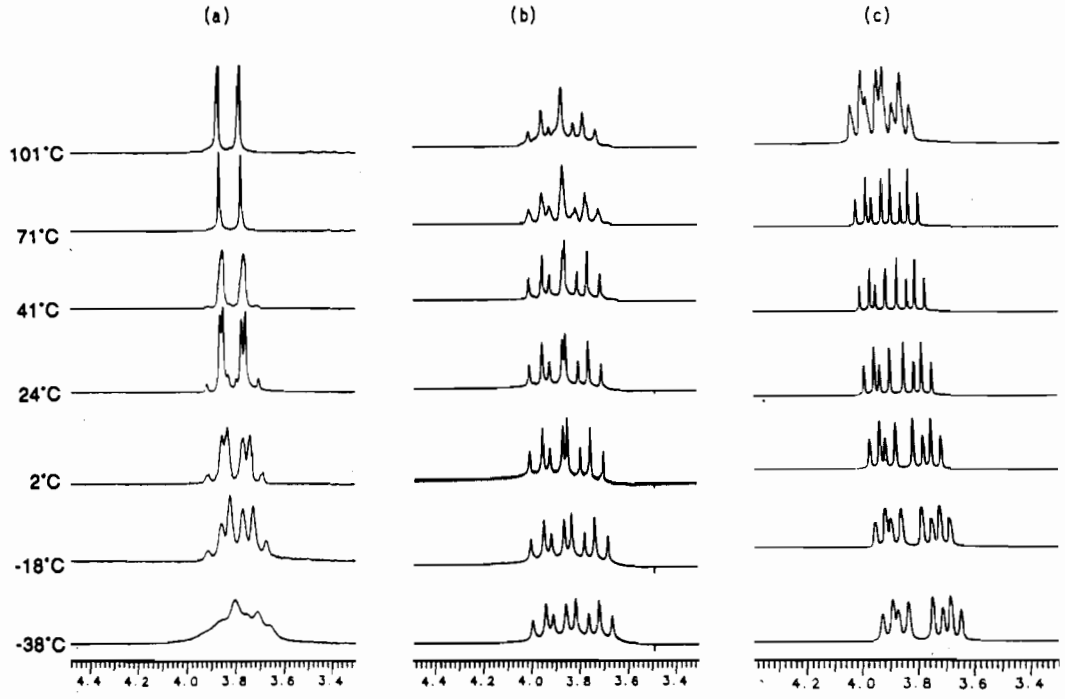

Figure 9. Comparison of the variable-temperature ^1H NMR spectra (ppm) for the methylene region of the phosphorinane rings of the thiophosphorane **2** recorded at 200 MHz (a), the oxyphosphorane **1** recorded at 200 MHz (b), and **1** recorded at 300 MHz (c), all in toluene-d_8 solutions.

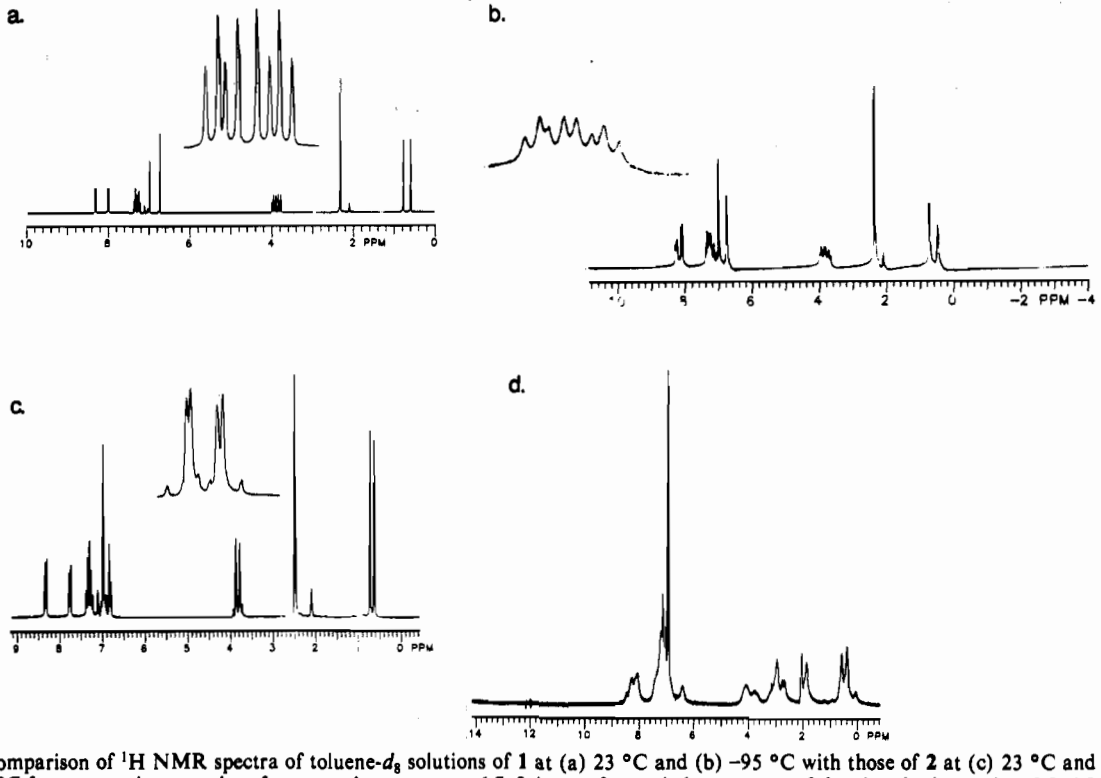

Figure 10. Comparison of ^1H NMR spectra of toluene-d_8 solutions of **1** at (a) 23 °C and (b) −95 °C with those of **2** at (c) 23 °C and (d) −95 °C. Signals at 23 °C from approximate regions for aromatic protons are 6.7–8.4 ppm; for methylene protons of the phosphorinane ring, 3.8–4.0 ppm (shown in an expansion as an inset in (a)–(c)); for xylyloxy methyl substituents, 2.3–2.5 ppm; and for phosphorinane ring methyl protons, 0.6–0.8 ppm. The signal between 2.0 and 2.1 ppm in all spectra results from toluene-d_8.

Thus, the sulfur derivative **2**, like **1**, undergoes a lower temperature Berry pseudorotation that equilibrates two of the four methylene protons but **2** also exhibits a higher temperature Berry pseudorotational process[29,30] that allows the equilibration of all four methylene protons. The placement of a five-membered oxygen-containing ring diequatorially in an exchange intermediate is a relatively high-energy process. Trippett[6] obtained an activation energy of 17.4 kcal/mol for this process for D, discussed in the Introduction. An unsaturated ring system, as present in **2**, would be expected to result in an even higher activation energy. The lack of evidence for this process in NMR spectra of the other phosphoranes studied that contain the dioxyphenanthrene group supports this assertion, especially when the closely related phosphorane **1** is examined (Figure 9). The implication is that the apicophilicity of the S–Xyl group is greater for some reason than that for the O–Xyl group. Previous NMR data by Trippett[6] indicate that the apicophilicities of OPh and SPh are similar in

(29) Houalla, D.; Wolf, R.; Gagnaire, D.; Robert, J. B. *J. Chem. Soc., Chem. Commun.* **1969**, 443.
(30) Reference 25, pp 163–165.

the compounds K and L. Perhaps with the larger ligands present in **2**, a steric factor is implicated.

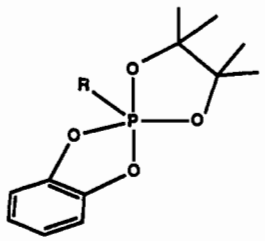

R	$\Delta G^{\ddagger}$ kcal/mol
PhO	20.5
PhS	20.7

K

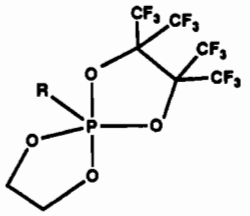

R	$\Delta G^{\ddagger}$ kcal/mol
PhO	17.4
PhS	17.3

L

In accompaniment of the process placing the five-membered ring diequatorially for **2**, one expects one proton signal for the methyl groups of the phosphorinane ring and one proton signal from the xylyl methyls. The latter is actually observed over the range from 100 to −60 °C. On lowering of the temperature to −95 °C, two broad signals emerge, indicating the cessation of xylyl group rotation. The two signals from the phosphorinane ring methyls observed at lower temperatures did not coalesce at the upper temperature limit reached, 100 °C. However, the chemical shift between the protons from these two methyl groups, which was 0.2 ppm at −95 °C, narrowed to 0.05 ppm at 100 °C. A higher temperature was not attained as peaks began to broaden, possibly due to the onset of decomposition.

The ^{1}H NMR data for the diazaphosphorinane derivative, **3**, is more difficult to interpret in terms of a ground-state structure in solution. The comparison of **1**, closely related to **2** in composition and X-ray structure, strongly suggests the presence of a solution structure in agreement with X-ray data on the solid state. For **2**, the changes in the ^{1}H NMR spectrum with temperature do not reasonably allow for a static structure having a ring located in diequatorial positions as the ground state. For derivative **3**, if we assume that the proton signals for the NCH_3 groups at 2.82 and 2.92 ppm represent a doublet as a result of $^3J_{P-H}$ coupling and that the NCH_2 multiplet at 3.32 ppm signifies one type of methylene group, then the NMR data are consistent with the presence of a solution-state structure in agreement with the solid-state X-ray structure with the proviso that rapid simple Berry pseudorotation is occurring. The NMR data by themselves, however, are consistent with a TBP with the nitrogen-containing ring located diequatorially.

For the trans-fused ring derivative, **4**, due to the lack of symmetry in the fused phosphorinane ring system, the presence of three kinds of proton signals attributed to two types of CH_2 protons and one type of CH proton of the six-membered ring is consistent with a ground-state TBP structure in solution that is in agreement with the X-ray structure. This structure may be undergoing exchange or not. Further, the NMR data are consistent with a TBP with the fused ring system located in diequatorial sites.

The ^{1}H NMR spectrum for the phenylphosphorane, **5**, which is invariant from −95 to 100 °C, is similar in analysis to that of **1**, and it follows that the same conclusion is reached regarding retention of the solid-state structure in solution, as already discussed for **1**.

Within the context of this and related work[2b,3-5] on cyclic oxyphosphoranes, we conclude that the solid-state structures invariably have rings located in apical–equatorial sites and that boat conformations in general result for six-membered saturated rings. Further, the presence of these structures in solution is strongly supported by variable-temperature NMR data for **1** and **2**, which undergo pseudorotational exchange processes. There is no reason to believe that the closely related oxyphosphorane derivatives **3–5** should not have similar solution structures with phosphorinane rings in apical–equatorial sites. The latter would agree with the X-ray structures found for **3** and **4**. The structural representations given in the Introduction for the newly synthesized trans-fused deoxythymidine derivative, **6**, and the cis-fused phosphorinane derivative, **7**, are given by analogy with the structures found for **1–4**. These conclusions are further supported by the recent solution NMR work of Yu and Bentrude[31] on the spirocyclic pentaoxyphosphorane M, which supported a twist conformation for the

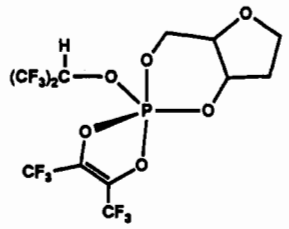

M

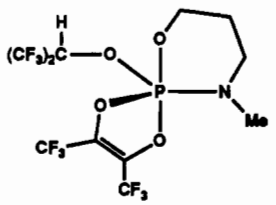

N

trans-fused dioxaphosphorinane ring located in apical–equatorial sites of a TBP, and by their related NMR work on the spirocyclic phosphorane N,[32] supporting a nonchair (boat and/or twist) conformation of the oxazaphosphorinane ring in a similar TBP.

They also have suggested that nonchair conformations for phosphorinane rings are their normal conformation.[31] We have fully characterized a variety of solid-state structures and find that boat or twist-boat conformations are the common structural entity for saturated six-membered dioxa- and diazaphosphorinane rings of oxyphosphoranes. However, as shown in another paper,[33] when hydrogen bonding is introduced in spirocyclic phosphoranes as an added feature, the structures of dioxaphosphorinane rings are more variable.

At present there are not definitive examples of cyclic oxyphosphoranes whose solid-state structures exhibit rings in diequatorial positions of a TBP. It is apparent from the present and related work that the introduction of a trans-fused ring (as in **4**) or heteroatoms attached to phosphorus of lower electronegativity than that for oxygen (as in **3** or E[3]) are not sufficient conditions to induce phosphorinane rings to orient in diequatorial positions of TBP. As a consequence, proposed phosphorane TBP models for enzymatic action on c-AMP that contain such ring orientations[8,9] are not supported by the present structural data, at least on the kinds of systems studied so far.

Acknowledgment. The support of this research by the National Science Foundation (Grant CHE88-19152) and the Army Research Office is gratefully acknowledged.

Supplementary Material Available: Tables of thermal parameters, additional bond lengths and angles, and hydrogen atom parameters (Tables S1–S3 for **1**, Tables S4–S6 for **2**, Tables S7–S9 for **3**, and Tables S10–S12 for **4**) (26 pages). Ordering information is given on any current masthead page.

(31) Yu, J. H.; Bentrude, W. G. *Tetrahedron Lett.* **1989**, *30*, 2195.
(32) Yu, J. H.; Bentrude, W. G. *J. Am. Chem. Soc.* **1988**, *110*, 7897.
(33) Day, R. O.; Kumara Swamy, K. C.; Fairchild, L. D.; Holmes, J. M.; Holmes, R. R. *J. Am. Chem. Soc.*, in press.
(34) (a) Yu, J. H.; Sopchik, A. E.; Arif, A. M.; Bentrude, W. G. *J. Org. Chem.* **1990**, *55*, 3444. (b) Yu, J. H.; Arif, A. M.; Bentrude, W. G. *J. Am. Chem. Soc.* **1990**, *112*, 7451.